PbZr0.52Ti0.48O3 and SrBi2Nb2O9 ferroelectric oxides integrated with YBa2Cu3O7 superconductor in multilayers epitaxially grown by pulsed laser deposition

Jean-René Duclere, Maryline Guilloux-Viry, A. Perrin, Caroline Soyer, Eric Cattan, Denis Remiens, A. Dauscher, Sébastien J. Weber, B. Lenoir

$PbZr_{0.52}Ti_{0.48}O_3$ and $SrBi_2Nb_2O_9$ ferroelectric oxides integrated with $YBa_2Cu_3O_7$ superconductor in multilayers epitaxially grown by pulsed laser deposition

J.R. Duclère, M. Guilloux-Viry, A. Perrin, C. Soyer[1], E. Cattan[1], D. Remiens[1], A. Dauscher[2], S. Weber[2] and B. Lenoir[2]

LCSIM, UMR 6511 du CNRS, Université de Rennes 1, Institut de Chimie de Rennes, Campus de Beaulieu, 35042 Rennes, France
[1] *MIMM Department, ZI du Champ de l'Abbesse, 59600 Maubeuge, France*
[2] *LPM, UMR 7556 du CNRS-UHP-INPL, École des Mines de Nancy, Parc de Saurupt, 54042 Nancy, France*

Abstract. Multilayers of $PbZr_{0.52}Ti_{0.48}O_3$ (PZT) or $SrBi_2Nb_2O_9$ (SBN) ferroelectrics (F) and $YBa_2Cu_3O_7$ (YBaCuO) superconductor (S) have been grown by pulsed laser deposition. F/S or S/F bilayers as well as S/F/S trilayers deposited on $SrTiO_3$ and MgO were epitaxially grown, as evidenced by x-ray diffraction (XRD) in θ-2θ and φ-scans modes, reflection high energy electron diffraction (RHEED) or electron channeling patterns (ECP). Superconducting YBaCuO films deposited on PZT exhibit a critical temperature, T_c, of about 86 K slightly below the value routinely obtained in the same deposition conditions on bare (100)$SrTiO_3$ substrate (typically 88-89 K). By contrast, the T_c of YBaCuO films on SBN, either on (100)$SrTiO_3$ or on (100)MgO is close to 88-89 K suggesting that SBN can be a good candidate as ferroelectric buffer layer for the growth of YBaCuO, especially on MgO for which a graphoepitaxial mechanism tends to limit the YBaCuO growth quality. In the case of F/S layers, hysteresis loops of PZT on YBaCuO show a saturated polarization larger than 30 $\mu C/cm^2$ and a coercive field of about 70 kV/cm. Secondary ion mass spectrometry (SIMS) experiments have been performed in order to correlate interdiffusion mechanisms with both structural data and physical properties.

1. INTRODUCTION

Oxide materials are of first importance for applications because of the abundance of properties, associated with similar structural characteristics allowing their integration in epitaxial heterostructures [1]. Combination of ferroelectrics and superconductors can be planned towards two goals : (i) conducting oxides provide electrodes for ferroelectric epitaxial growth, and (ii) ferroelectrics give access to tunable superconductor devices. C-axis oriented $YBa_2Cu_3O_7$ (YBaCuO) thin films are of prime interest because of low microwave losses, illustrated by low surface resistance value, providing a substantial loss reduction over identical circuits fabricated from normal metals [2]. Ferroelectrics as $PbZr_{0.52}Ti_{0.48}O_3$ (PZT) or $SrBi_2Nb_2O_9$ (SBN) presenting polarization along c axis and ab plane, respectively, are intensively studied in view of applications in Fe-RAM for instance [3]. Moreover, Aurivillius phases like SBN are fatigue free when cycled [4]. In this frame, we report on several heterostructures integrating PZT or SBN and YBaCuO *in situ* epitaxially grown by pulsed laser deposition. YBaCuO/PZT/YBaCuO/(100)$SrTiO_3$, YBaCuO/SBN on both (100)$SrTiO_3$ and (100)MgO, PZT/YBaCuO/(100)$SrTiO_3$, and SBN/YBaCuO/(110)$SrTiO_3$ multilayers were epitaxially grown as evidenced by x-ray diffraction (XRD) in θ-2θ and φ-scans modes, reflection high energy electron diffraction (RHEED). Ferroelectric and superconducting behaviours have been evaluated in the various structures.

2. EXPERIMENTAL

Thin films have been grown by pulsed laser deposition (λ = 308 nm, 2Hz, 3,5 J/cm^2) from home-made sintered targets on heated substrates in oxygen atmosphere, using a multitarget holder allowing the *in situ* deposition of multilayers. Deposition conditions for the different layers are summarized in table 1.

Table 1 : Deposition parameters for each material in the various heterostructures

Material	PZT	SBN	YBaCuO on $SrTiO_3$, and SBN	YBaCuO on PZT
Target	$PbZr_{0.52}Ti_{0.48}O_3$	$SrBi_2Nb_2O_9$ + 30% Bi_2O_3	$YBa_2Cu_3O_7$	$YBa_2Cu_3O_7$
Deposition temperature	560° C	700° C	720° C	700° C
Oxygen pressure	0.5 mbar	0.3 mbar	0.3 - 0.5 mbar	0.5 mbar

The phase analysis and growth direction of the films were determined by θ-2θ X-ray diffraction (XRD). In-plane ordering was qualitatively checked by reflection high energy electron diffraction (RHEED). Epitaxial relationships were established by XRD φ-scans with a four-circle texture diffractometer. The in-depth distribution of the different elements was analysed using SIMS (VG SIMSLAB) in SNMS mode. The SNMS (Secondary Neutral Mass Spectrometry) method, based on post-ionization of neutral particles flux emitted from the sample surface is applied to get these profiles. Primary Ar^+ ions (8 kV, 300 nA) were scanned over a sample area of 250*250 μm^2.

The ferroelectric loops P(E) were measured using a standard Radian RT6000. The charge option of RT6000 was used, the top electrode was always connected to the drive terminal of the test equipment, while the bottom electrode was connected to the return terminal. Superconducting critical temperature, T_c, was determined from a.c. susceptibility transition (119 Hz).

3. RESULTS

3.1 Structural characteristics

As expected from the good lattice constant mismatch between the various materials (table 2) epitaxial multilayers have been achieved for PZT-YBaCuO and SBN-YBaCuO bilayers grown on $SrTiO_3$ as well as on MgO.

Table 2 : Lattice constant mismatch values Δa/a between the materials under study

	$SrTiO_3$	MgO	YBaCuO
c-axis oriented PZT	3.3 %	4.0 %	3.9 %
c-axis oriented SBN*	0.1 %	7.4 %	0.54 %

* in-plane axes along the diagonals of the substrate

3.1.1 PZT-YBaCuO heterostructures

Taking into account that c-axis YBaCuO films are required for both microwave applications and polarization of PZT along c-axis, PZT/YBaCuO/(100)$SrTiO_3$, YBaCuO/PZT/(100)$SrTiO_3$, and YBaCuO/PZT/YBaCuO/(100)$SrTiO_3$ have been prepared. C-axis orientation was evidenced by θ-2θ X-ray diffraction. Whereas narrow rocking curves values Δθ (full width at half maximum of θ-scan), lower than 0.2° were measured on 001 peaks of PZT or YBaCuO on bare $SrTiO_3$, in bilayers like PZT/YBaCuO, Δθ ~ 0.3° and ~ 0.8° were measured on YBaCuO and PZT layers, respectively, and a value of about 0.9° was measured for each material in trilayers, evidencing low mosaïcity effects. The in-plane orientation in bi- and trilayers , *i.e.* the epitaxial growth, was confirmed by RHEED patterns, showing narrow streaks.

3.1.2 SBN -YBaCuO heterostructures

For superconducting purpose, YBaCuO/SBN bilayers were grown on (100)$SrTiO_3$ and (100)MgO, the latter substrate being suitable for microwave applications. In contrast, since the polarization vector of SBN lies in the ab plane, SBN/YBaCuO structures were deposited on (110)$SrTiO_3$ in order to obtain a non-zero resulting polarization along the perpendicular to the surface.

YBaCuO/SBN are c-axis oriented on (100) substrates, as evidenced by θ-2θ XRD. Shoulders observed on some (00l) SBN peaks can be explained by an intergrowth mechanism related to Bi deficiency [6]. The presence of some weak unidentified peaks suggests the existence of a secondary phase which could be due to interdiffusion (see section 3.2). The high quality of c-axis orientation is confirmed by low Δθ values, typically smaller than 0.5° on (100)$SrTiO_3$, and slightly larger on MgO (up to 1.5-2° on 15*15 mm^2 substrates), probably in relation with larger mismatch for this substrate (table 2). The in-plane order proving the epitaxial growth was analysed by x-ray φ-scans (figure 1). Indeed, four peaks are displayed at the same azimuths for SBN, YBaCuO and MgO. Moreover, four additional peaks are visible on the YBaCuO pattern, the signature of the coexistence of two in-plane orientations at 45° from each other. The occurence of the minor orientation was evaluated from the XRD peaks intensity to about 3 %.

Structural characteristics of YBaCuO on (110)$SrTiO_3$ were previously studied [5]. A (116) orientation of epitaxial SBN on (103)YBaCuO is achieved, as evidenced by θ-2θ x-ray diffraction and fully confirmed by x-ray φ-scans. As in the case of the above YBaCuO/SBN bilayers on (100)$SrTiO_3$, unidentified peaks were observed, but at different diffraction angles. We can suppose that this secondary phase is the same in the two cases and similarly oriented with respect to YBaCuO and/or SBN : in fact θ-2θ XRD performed in standard geometry (ψ = 0°) on the layers grown on (110)$SrTiO_3$ and at ψ = 47° in the case of the c-axis multilayer, show the same peaks at 2θ = 29.45° and 31° ($CuK_{\alpha 1}$ radiation).

Δθ values measured for the 2212 peak of SBN and 103 peak of YBaCuO, are typically about 1°. The corrugated surface of epitaxial 116 SBN is revealed by spotty RHEED patterns, contrasting with the one of 00l film formed by narrow streaks. This is the signature of a rough surface at an atomic scale, which is quite similar to the previously reported behaviour of (103)YBaCuO films [5].

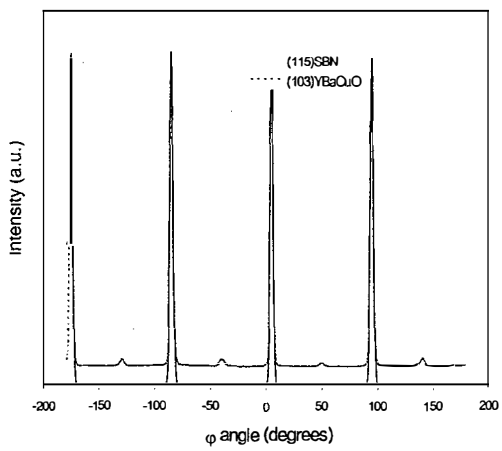

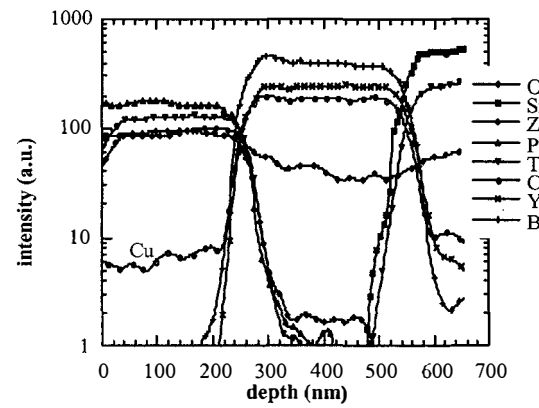

Figure 1 : φ-scans on the 103 and 115 reflections of YBaCuO and SBN, respectively, in YBaCuO/SBN/(100) MgO systems (left)
Figure 2 : SIMS profile on a PZT/YBaCuO/(100)$SrTiO_3$ heterostrucure (right)

3.2 SIMS analyses

As mentioned above, X-ray diffraction performed on PZT-YBaCuO bilayers did not evidence any secondary phase. In agreement with this result, SIMS profile (figure 2) show quite sharp interfaces between PZT and YBaCuO, whatever is the stacking order, suggesting that there is no strong interaction between the two materials under our deposition conditions. However, we can observe that the Cu signal from YBaCuO does not fall to zero in PZT suggesting some Cu diffusion in PZT.

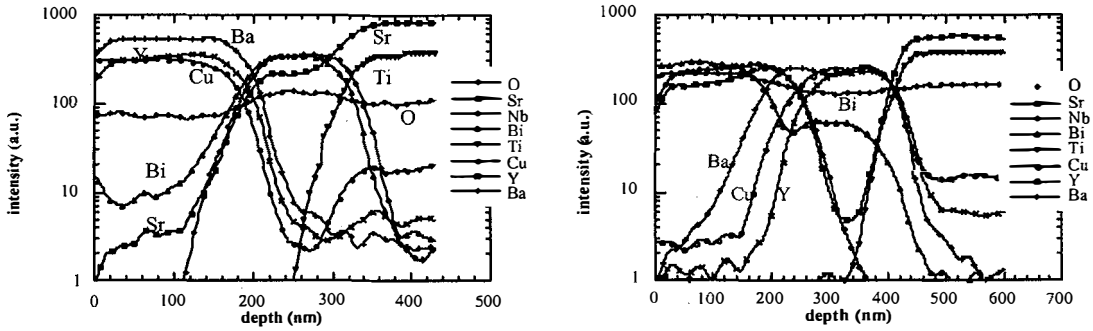

Figure 3 : SIMS profiles on (a)YBaCuO/SBN/(100)$SrTiO_3$ and (b)SBN/YBaCuO/(110)$SrTiO_3$ heterostrucures

In contrast, SIMS profiles observed for the SBN – YBaCuO bilayers (figure 3) evidence strong interdiffusion : in particular Bi diffuses strongly in the YBaCuO bottom layer and Ba and Cu signals suggest a diffusion of these elements in SBN (figure 3 b). These results are in good agreement with the merging of additional peaks on XRD patterns. Up to now the associated secondary phases were not identified. SIMS results corresponding to the films prepared in our conditions differ from the chemical interactions of Zr or Ti from PZT and Nb from SBN with Ba from YBaCuO previously suggested by Y.A. Boikov et al. [7]. In spite of interdiffusion evidenced in some cases, the good uniformity in the top layer is systematically evidenced by flat signals on the SIMS profiles.

3.3. Ferroelectric measurements

The ferroelectric behaviour of PZT and SBN on YBaCuO/$SrTiO_3$ sublayer has been checked by electrical measurements. Figure 4 shows the hysteresis loop of a PZT film epitaxially grown on YBaCuO, using a Pt top electrode deposited by a lift-off process. The saturated polarization larger than 30 $\mu C/cm^2$ and a coercive field of about 70 kV/cm are close to values reported for this type of structure [8,9]. Work is now in progress to measure the remnant polarization of (116)SBN/(103)YBaCuO. Preliminary measurements allowed to evidence the ferroelectric behaviour, but experimental difficulties to take electrical contacts were encountered to measure the actual hysteresis loop.

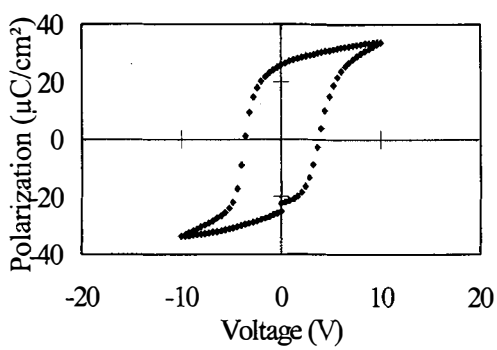

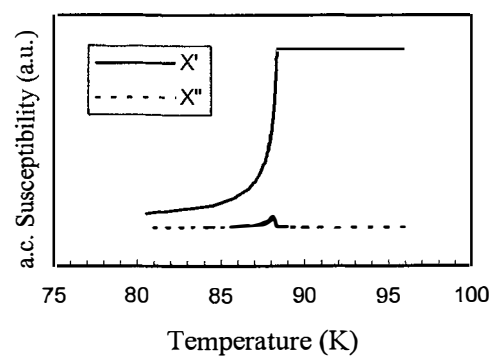

Figure 4 : Hysteresis loop of a PZT/YBaCuO/(100)$SrTiO_3$ heterostructure (left)
Figure 5 : Superconducting transition of a 15*15 mm^2 YBaCuO/SBN/(100)MgO film (right)

3.3. Superconducting behaviour

In spite of the absence of significant diffusion of PZT in YBaCuO, a slight decrease of the critical temperature of YBaCuO has been observed : typically a narrow transition was recorded at about 86-87 K instead of 88-89 K on bare $SrTiO_3$. As a similar decrease of T_c was also observed when YBaCuO single layers were deposited between PZT deposition runs in the same chamber, we initially assumed some lead contamination effect, in relation with the Pb oxide volatility. However, up to now, no lead has been detected in YBaCuO, in agreement with SIMS results.

In contrast, figure 5 illustrates the superconducting transition of YBaCuO which was routinely observed on SBN/(100)MgO as well as on SBN/(100)$SrTiO_3$ at T_c around 88.5 K. Moreover, the area under the χ " peak (S(χ ")), a measurement of low frequency losses and which is strongly correlated to microwave losses [10], is in agreement with the low mixture of the two in-plane orientations (3 %) of the c-axis YBaCuO we have previously reported in the case of YBaCuO/MgO [10]. Then, the observed value of S(χ ") would imply a low surface resistance (smaller than 2 mΩ). Work is in progress to directly measure the microwave surface resistance of such sample.

4. CONCLUSION

As expected from structural considerations, epitaxial multilayers integrating YBaCuO, SBN and PZT were grown by pulsed laser deposition. SIMS experiments associated with XRD evidence interdiffusion mechanisms in several cases. According to these results and to the ferroelectric and superconducting measurements, YBaCuO appears to be a good candidate as an electrode for PZT, while SBN seems a promising seed layer for the control of high quality superconducting epitaxial YBaCuO, especially on MgO substrate. The suitability of this heterostructure for microwave applications will be evaluated. The complementarity of PZT/YBaCuO and SBN/YBaCuO on (100)$SrTiO_3$ is illustrated. Indeed, the control of both heterostructures would give access to a standard capacitor geometry (using the c-axis polarization of PZT) or to a coplanar geometry (using the a-axis polarization of SBN).

Acknowledgments

This work has been supported in part by a CNRS-Région Bretagne grant and by CNRS in the frame of "Materials Program". φ-scan XRD have been made in Metallurgy Laboratory of INSA, Rennes. Langlois Fundation is acknowledged for partial financial support.

References

1. M. Suzuki, T. Ami, Mater. Sci. & Eng B **41**, 166 (1996)
2. « Special issue on microwave applications of superconductivity » , IEEE Trans. Microwave Theory Tech., **MTTT-39**, No 9, (1991)
3. For an overview, « Electroceramic thin films », Part II, MRS Bull. **21**, No 7, (1996)
4. C.A-Paz de Araujo, J.D. Cuchlaro, L.D. McMillan, M.C. Scott, J.F. Scott, Nature, **374**, 627, (1995)
5. M. Guilloux-Viry, C. Thivet, A. Perrin, M. Sergent, M.G. Karkut, C. Rossel, A. Catana, J. Cryst. Growth, **132**, 396, (1993)
6. J.R. Duclère, M. Guilloux-Viry , A. Perrin, J.Y. Laval, Appl. Surf. Sci., in press
7. Y.A. Boikov, Z.G.Ivanov, E. Olsson, T. Claeson, Physica C, **282-287**, 111, (1997)
8. Y.A. Boikov, S.K. Esayan, Z.G.Ivanov, G. Brorsson, T. Claeson, J. Lee, A. Safari, Appl. Phys. Lett., **61**, 528, (1992)
9. J. Lee, L. Johnson, A. Safari, R. Ramesh, T. Sands, H. Gilchrist, V.G. Keramidas, Appl. Phys. Lett, **63**, 27, (1993)
10. X. Castel, M. Guilloux-Viry, A. Perrin, C. Le Paven-Thivet, J. Debuigne, Physica C, **255**, 281, (1995).